Heliyon 10 (2024) e38062

Contents lists available at ScienceDirect

Heliyon

journal homepage: www.cell.com/heliyon

Research article

Amide proton transfer and apparent diffusion coefficient analysis reveal susceptibility of brain regions to neonatal hypoxic-ischemic encephalopathy

Yu Guo [a,b], Xiaohu Zhu [a,b], Jian Li [a,b], Baiqi Zhu [a,b], Yajing Ye [a,b], Xuehua Peng [a,b,*]

[a] *Department of Radiology, Wuhan Children's Hospital(Wuhan Maternal and Child Healthcare Hospital), Tongji Medical College, Huazhong University of Science & Technology, China*
[b] *Wuhan Clinical Research Center for Children's Medical Imaging, China*

A R T I C L E I N F O

Keywords:
Amide proton transfer
Apparent diffusion coefficient
Hypoxic-ischemic encephalopathy
Neonate

A B S T R A C T

Purpose: To identify brain regions affected by Hypoxic-Ischemic Encephalopathy (HIE) in neonates using Amide Proton Transfer (APT) imaging and Apparent Diffusion Coefficient (ADC).
Materials and methods: Twenty neonates were divided into HIE and control groups. All neonates were undergoing MRI, including APT and DWI. Imaging analysis was performed using SPM12. The independent-samples *t*-test was used to analyze the difference in APTw values and ADC values between the mild HIE neonates and the control group. The receiver operating characteristic (ROC) curves were established to assess the diagnostic values of APTw and ADC values in different brain regions for HIE. Pearson's correlation analysis was used to analyze the correlation between APTw values and ADC values for each region.
Results: APTw values were significantly higher in 26 regions of the HIE group. ADC values were lower in the right anterior temporal lobe and higher in bilateral Subthalamic nucleus in HIE. The APTw values of 22 regions showed very high area under the curve (AUC), whereas the AUC of ADC values in right anterior temporal lobe and right subthalamic nucleus were both 0.802. Notably, the right anterior temporal lobe exhibited significant differences in both APTw and ADC values between the HIE and control groups, additionally, APTw value was significant positive correlated with ADC values in right anterior temporal lobe.
Conclusion: APTw and ADC are effective in detecting HIE, with APTw being more sensitive. The right anterior temporal lobe is particularly affected by HIE, with significant changes in APTw and ADC values and a positive correlation between them. This suggests that temporal lobe damage may be critical in the long-term neurological consequences of HIE.

Abbreviations: HIE, Hypoxic-Ischemic Encephalopathy; APT, Amide Proton Transfer; ADC, Apparent Diffusion Coefficient; DWI, Diffusion-weighted imaging; ROC, receiver operating characteristic; AUC, under the curve; T1WI, T1 weighted imaging; T2WI, T2 weighted imaging; T2 FLAIR, T2 Fluid Attenuated Inversion Recovery; APTw, APT weighted.

* Corresponding author. Department of Radiology, Wuhan Children's Hospital (Wuhan Maternal and Child Healthcare Hospital), Tongji Medical College, Huazhong University of Science and Technology, Wuhan, 430016, Hubei, China.
E-mail address: wchradiology@163.com (X. Peng).

https://doi.org/10.1016/j.heliyon.2024.e38062
Received 23 June 2024; Received in revised form 26 August 2024; Accepted 17 September 2024
Available online 19 September 2024

1. Introduction

Neonatal hypoxic ischaemic encephalopathy (HIE) is a disease caused by insufficient oxygen supply to the brain tissue or reduced cerebral blood flow [1], and is the most common neurological disease in the neonatal period, causing early neonatal death and long-term neurological dysfunction [2]. Globally, approximately 814,000 newborns die from HIE each year [3], with 25 % of affected children suffering permanent neurological deficits [4], significantly impacting the health and future quality of life of newborns. Many studies have found that children with mild HIE may present with neurological impairments in school age and beyond, with approximately 70 % of affected children experiencing behavioral and learning difficulties that significantly impact their daily lives [2]. Therefore, identification of brain regions damaged by neonatal HIE is important for investigating the neuropathological mechanisms of HIE and providing appropriate therapeutic strategies.

Magnetic resonance imaging (MRI) as a biomarker of neurodevelopmental prognosis of HIE has been widely used in clinical practices. There has been a growing trend towards defining quantitative MR biomarkers, such as the Diffusion-weighted imaging (DWI), proton (1H) MR spectroscopy (MRS), and conventional MR scoring systems, with the aim of enhancing prognostic objectivity [5]. DWI is a commonly used neuroimaging technique that reflects the microscopic diffusion movement of water molecules and is used to assess the microscopic structural changes of brain tissue [6]. Diffusion-weighted imaging (DWI) is more sensitive to brain injury caused by hypoxic-ischemic encephalopathy (HIE) than conventional MRI, and its application in the detection of HIE has been on the rise [4,6,7]. The signal intensity of DWI is quantified by the apparent diffusion coefficient (ADC). Some studies have shown that changes in ADC values in the basal ganglia and thalamus of children with HIE are strongly associated with prognosis. Some researchers have suggested that a significant decrease ADC values in pontine and cerebellum represent a poor prognosis [8].

Amide proton transfer (APT) imaging is a novel imaging technique that has shown promise in the evaluation of brain injury in neonates with HIE [9–11]. Variations in APT may reflect changes in whole brain metabolism due to perinatal hypoxia-ischemia [12]. APT-weighted (APTw) signal intensity reflects the content of endogenous proteins and peptides as well as the rate of amino proton exchange in biological tissues, and can indirectly measure the pH level and protein concentration in tissues [13], providing us with more valuable information about tissue metabolism and cellular integrity. APT enhances the multidimensional comprehension of the disease process and is anticipated to bear clinical relevance in the diagnosis, treatment, and prognosis of neonatal HIE.

ADC reflects the diffusion of intracellular water and is commonly used to identify areas of acute ischemia [6,14]. In contrast, APTw imaging sensitively captures changes in the brain's microenvironment [10]. The pathophysiology of HIE is highly complex. Therefore, we will leverage the strengths of both ADC and APTw to comprehensively quantify the signal changes in the brains of HIE patients. Our goal is to identify potential neuroimaging biomarkers in neonatal HIE.

2. Materials and Methods

The study was ethically approved by the Ethics Committee of Wuhan Children's Hospital (2021R109-E03). Written informed consent was obtained from the parents of the participants prior to the examinations.

2.1. Participants

The data collection period spanned from May 2021 to December 2023 at our hospital. Twenty neonates were selected, we divided the neonates into an HIE group and a control group based on their clinical history.

Our inclusion criteria of HIE group comprise: (1) History of intrauterine distress or perinatal asphyxia; (2) independent grading of encephalopathy by two neonatologists according to modified Sarnath criteria [15]; (3) underwent conventional cranial MRI within 1 month after birth, which showed no significant abnormalities; (3) performed APT and DWI.

The inclusion criteria of control group comprise: (1) no history of fetal intrauterine distress or perinatal asphyxia; (2) no neurological diseases; (3) performed conventional cranial MRI within one month after birth, without any significant abnormalities; (4) underwent both APT and DWI.

2.1.1. MR protocols

All newborns underwent the scans during natural sleep. Scans were performed on a 3 T MRI scanner (Ingenia; Philips Healthcare, Best, the Netherlands), using a 32-channel sensitivity–encoding head coil.

Conventional MRI includes T1 weighted imaging (T1WI), T2weighted imaging (T2WI) and T2 Fluid Attenuated Inversion Recovery (T2 FLAIR). In addition, all newborns were also scanned DWI and APT. For simplicity, T1WI (TR: 2000 ms; TE: 30 ms; slice thickness: 4.5 mm; gap 0.8 mm), T2WI (TR: 3500 ms; TE: 130 ms; slice thickness: 4.5 mm; gap 0.8 mm), and T2 FLAIR (TR: 8500 ms; TE: 155 ms; TI: 2450 ms; slice thickness: 4.5 mm; gap 0.8 mm) sequences would be referred to as conventional MRI.

APT imaging was performed with a fat–suppression, 3D TSE-Dixon pulse sequence. The parameters were as follows: TR/TE: 6491/8.3 ms; field-of-view (FOV): 180 × 122 × 70 mm3; voxel size: 1.8 × 1.8 × 5 mm3; matrix: 100 × 68; scan duration: 240 s. DWI utilised the EPI sequence with TR/TE: 4000/103 ms; and b factor 1000 s/mm2. The APT weighted (APTw) image and ADC map were generated by the post-processing workstations.

2.1.2. Imaging analysis

We used Statistical Parametric Mapping 12 (SPM12) and MATLAB for analyzing neonatal APT and ADC data. Preprocessing included motion correction, co-registration, smoothing, and brain masking. T2 structural data was segmented with SPM8, and APTw

images were normalized using the T2 segmentation transformation matrix. Brain tissue classification used the "ALBERTs atlas," which automatically segments neonatal brain MR images into 50 regions of interest (ROIs) [16,17]. These ROIs segmented the registered APT maps for group analysis.

2.1.3. Statistical analysis

The statistical analyses were completed by SPSS 25.0 software. The measurement data were expressed as mean ± standard deviation (x ± s) for accuracy and clarity. The difference in APTw values and ADC values between the mild HIE neonates and the control group was analyzed with the independent-samples *t*-test. The diagnostic performance of significant APTw and ADC value for differentiating mild HIE from control group was assessed by using receiver operating characteristic (ROC) curve with the area under the curve (AUC), and the diagnostic sensitivity and specificity of APTw and ADC values in different brain regions were identified based on Youden index. The correlation between APT values and ADC values for each region was analyzed by Pearson's correlation analysis. $P < 0.05$ indicated statistically significant difference.

3. Results

3.1. Clinical characteristics

There are 12 newborns in the HIE group, with 6 boys and 6 girls. Their gestational ages at birth were in the range of 34–39 weeks, with an average of 35.23 ± 1.57 weeks, the gestational ages at scan were 36.89 ± 2.39 weeks. Birth weights were 2.66 ± 0.72 kg. The control group included 8 neonates (1 males and 7 females). Their gestational ages at birth were 39.09 ± 0.84 weeks, the gestational ages at scan were 41.05 ± 1.71 weeks. Birth weights were 3.56 ± 0.53 kg.

3.2. APTw and ADC values in neonatal HIE vs. control groups

We showed the conventional MRI, ADC and APTw images of the group of HIE and controls (Fig. 1) and template-based ROI segmentation (Fig. 2). APTw values in all brain regions were elevated in the HIE group compared to the control group. There were 26 brain regions with elevated APTw values in the HIE group. These brain regions were the right hippocampus, bilateral amygdala, bilateral caudate nucleus, bilateral lentiform Nucleus, bilateral temporal lobes, bilateral frontal lobes, right parietal lobe, left insula, left occipital lobe, parahippocampal posterior gyrus, occipitotemporal postero-lateral gyrus, posterior medial-inferior temporal gyrus, anterior medial-inferior temporal gyrus, bilateral cerebellums, brainstems, left posterior cingulate gyrus, and left ventricle (Table 1).

ADC values showed a different kind of pattern from APTw values in the HIE and control groups. In the HIE group, ADC values were significantly lower in the right anterior temporal lobe than in the control group; bilateral Subthalamic nucleus were significantly higher (Table 2).

3.3. ROC curve analysis of APTw and ADC values in neonatal HIE

We analyzed the brain regions with significant variation there by performing ROC curves. The results of the ROC curves for APTw and ADC values are shown in Tables 3 and 4 respectively. 22 brain regions were statistically significant, and most of them had an area under the curve greater than 0.8. The ROC curve results of ADC values showed significant differences in the right anterior temporal

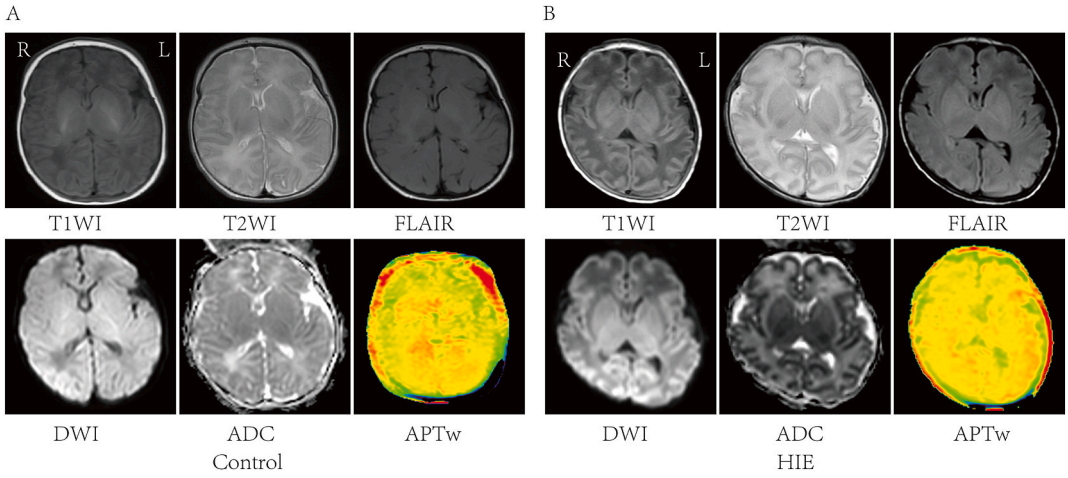

Fig. 1. Conventional MRI, ADC and APTw images of the group of HIE and controls. A. A 7-day-old girl, born at gestational week 39^{+2}, was presented with jaundice, and cranial MRI results showed no significant abnormality; B. A 22-day-old boy, with a gestational week of 31 at birth, was diagnosed with mild HIE.

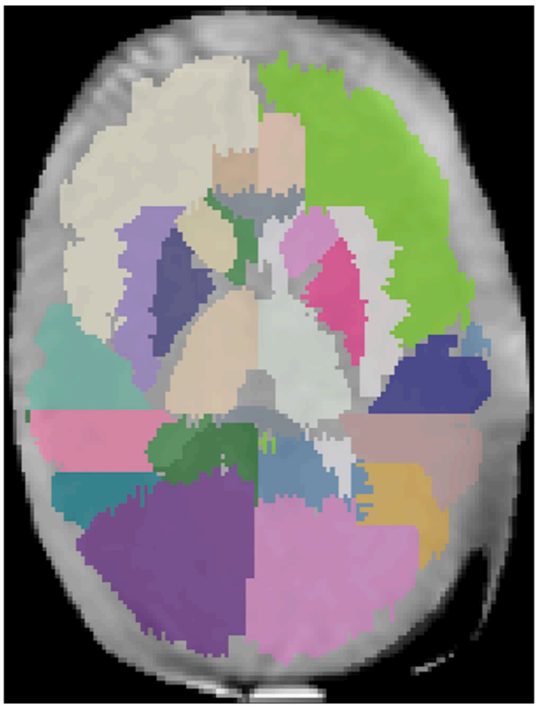

Fig. 2. Template-based ROI segmentation APTw image as an example of ROI segmentation based on neonatal brain templates.

Table 1
Brain regions with significant APTw Values in Neonatal HIE vs. Control Groups.

	Control	HIE	t	*p*
Right Hippocampus	2.871 ± 0.14	3.216 ± 0.333	−3.193	0.006
Right Amygdala	2.316 ± 0.149	2.841 ± 0.49	−2.914	0.009
Left Amygdala	2.173 ± 0.14	2.492 ± 0.421	−2.44	0.029
right Anterior temporal lobe, medial part	1.996 ± 0.227	2.478 ± 0.315	−3.72	0.002
Left Anterior temporal lobe, medial part	1.75 ± 0.163	2.588 ± 0.338	−7.39	0.0001
right Anterior temporal lobe, lateral part	2.048 ± 0.242	2.638 ± 0.415	−4.01	0.001
Left Anterior temporal lobe, lateral part	2.091 ± 0.229	2.648 ± 0.323	−4.2	0.001
Left Medial and inferior temporal gyri anterior part	2.792 ± 0.418	3.29 ± 0.387	−2.7	0.014
Right Cerebellum	2.136 ± 0.169	2.735 ± 0.506	−3.8	0.002
Left Cerebellum	2.165 ± 0.238	2.848 ± 0.393	−4.39	0.0001
Brainstem	2.028 ± 0.274	2.55 ± 0.279	−4.14	0.001
Left Insula	2.363 ± 0.239	2.721 ± 0.455	−2.0	0.057
Left Occipital lobe	2.411 ± 0.302	3.127 ± 0.446	−3.96	0.001
Left Gyri parahippocampalis et ambiens posterior part	2.527 ± 0.309	3.046 ± 0.337	−3.48	0.003
right Gyri parahippocampalis et ambiens posterior part	2.495 ± 0.296	3.053 ± 0.665	−2.22	0.04
Left Lateral occipitotemporal gyrus, gyrus fusiformis posterior part	2.483 ± 0.274	2.956 ± 0.477	−2.53	0.021
Right Lateral occipitotemporal gyrus, gyrus fusiformis posterior part	2.485 ± 0.343	3.481 ± 0.434	−5.44	0.0001
Left Cingulate gyrus, posterior part	2.3 ± 0.43	2.842 ± 0.629	−2.12	0.048
Left Frontal lobe	2.479 ± 0.353	3.079 ± 0.357	−3.7	0.002
Right Frontal lobe	2.363 ± 0.266	2.972 ± 0.415	−3.67	0.002
Right Parietal lobe	2.45 ± 0.328	3.292 ± 0.502	−4.17	0.001
Left Caudate nucleus	2.349 ± 0.472	3.045 ± 0.428	−3.43	0.003
Right Caudate nucleus	2.458 ± 0.266	3.148 ± 0.407	−4.58	0.0001
Left Lentiform Nucleus	2.427 ± 0.305	2.748 ± 0.341	−2.15	0.046
Right Lentiform Nucleus	2.178 ± 0.445	2.876 ± 0.391	−3.71	0.002
left Lateral Ventricle	2.497 ± 0.301	3.399 ± 0.916	−3.16	0.007

lobe and the right subthalamic nucleus, with AUCs greater than 0.8.

3.4. Correlation analysis of APTw and ADC values in neonatal HIE

We performed a correlation analysis of APTw and ADC values in various brain regions of the HIE group. Our results showed

Table 2
Brain regions with significant ADC Values in Neonatal HIE vs. Control Groups.

	Control	HIE	t	*p*
right Anterior temporal lobe, medial part	1.034 ± 0.346	0.588 ± 0.452	2.359	0.03
left Subthalamic nucleus	1.049 ± 0.254	1.296 ± 0.229	−2.269	0.036
Right Subthalamic nucleus	1.052 ± 0.485	1.557 ± 0.368	−2.652	0.016

ADC: $*10^{-3}$ mm^2/s.

Table 3
The diagnostic efficiency test of brain regions with significant APTw Values in Neonatal HIE.

	AUC (95%CI)	CUT-OFF	*p*
Amygdala right	0.854 (0.686–1)	2.673	0.009
Anterior temporal lobe, medial part right	0.896 (0.757–1)	2.088	0.003
Anterior temporal lobe, lateral part right	0.865 (0.702–1)	2.665	<0.001
Anterior temporal lobe, lateral part left	0.906 (0.775–1)	2.404	0.007
Medial and inferior temporal gyri anterior part left	0.823 (0.617–1)	2.944	0.003
Cerebellum right	0.854 (0.681–1)	2.523	0.017
Cerebellum left	0.938 (0.836–1)	2.664	0.009
Brainstem, spans the midline	0.917 (0.797–1)	2.412	0.001
Insula left	0.771 (0.551–0.99)	2.714	0.002
Occipital lobe left	0.865 (0.705–1)	3.084	0.045
Gyri parahippocampalis et ambiens posterior part left	0.865 (0.687–1)	2.678	0.007
Gyri parahippocampalis et ambiens posterior part right	0.781 (0.577–0.986)	3.016	0.007
Lateral occipitotemporal gyrus, gyrus fusiformis posterior part left	0.802 (0.584–1)	2.562	0.037
Lateral occipitotemporal gyrus, gyrus fusiformis posterior part right	0.969 (0.901–1)	3.105	0.025
Frontal lobe left	0.906 (0.774–1)	2.645	0.001
Frontal lobe right	0.927 (0.78–1)	2.523	0.003
Parietal lobe right	0.938 (0.826–1)	2.803	0.002
Caudate nucleus left	0.885 (0.738–1)	2.746	0.001
Caudate nucleus right	0.927 (0.797–1)	2.781	0.004
Lentiform Nucleus right	0.927 (0.814–1)	2.701	0.002
Corpus Callosum	0.802 (0.6–1)	2.862	0.002
Lateral Ventricle left	0.833 (0.639–1)	2.87	0.025

Table 4
The diagnostic efficiency test of brain regions with significant ADC Values in Neonatal HIE.

	AUC (95%CI)	CUT-OFF	*p*
Anterior temporal lobe, medial part right	0.802 (0.606–0.998)	0.642	0.025
Subthalamic nucleus right	0.802 (0.577–1)	1.196	0.025

ADC: $*10^{-3}$ mm^2/s.

meaningful correlations between APTw values and ADC values in these brain regions: right anterior temporal lobe ($r = 0.621$, $p = 0.031$), left posterior hippocampal parahippocampal gyrus ($r = 0.641$, $p = 0.025$), left posterior medial temporal-subcentral gyrus ($r = -0.768$, $p = 0.004$), and bilateral Subthalamic nucleus (left: $r = -0.685$, $p = 0.014$; right: $r = -0.618$, $p = 0.032$).

In summary, we found that the right anterior temporal lobe was significantly different in both APTw and ADC in the comparison between the HIE and control groups, and there was a significant positive correlation between the APTw and ADC values in the right anterior temporal lobe.

Combining the above results, we found that both APTw and ADC values of the right anterior temporal lobe were significantly changed in the HIE group. Meanwhile, the APTw value and ADC value of right anterior temporal lobe were significantly positively correlated. This result prompts us that changes in the right anterior temporal lobe may have a very crucial role in the neuropathophysiology of HIE.

4. Discussions

HIE is a syndrome of neonatal brain dysfunction caused by perinatal asphyxia. Cerebral hypoxic-ischemic can lead to disturbances in energy metabolism, while infant brain development requires a large amount of energy. This can cause cellular edema and alter protein and pH levels in the brain. DWI shows cytotoxic edema extent, while APT reveals pH changes in lesions. Therefore, we use APT and DWI to evaluate the brains of neonates with HIE, tracing pathophysiological processes from the internal tissue environment, helping us to understand the disease process more comprehensively, and providing more detailed information for diagnosis and treatment.

In our study, the elevated APTw values in various brain regions of the HIE group compared to the control group. A previous study

analyzed cranial APT in neonates with HIE, and APTw values were also elevated in most brain regions, similar to our findings [9]. In another study, APT values in the bilateral caudate nucleus, bilateral pallidum/shell nuclei, and bilateral thalamic and brainstem regions were found to be positively and linearly correlated with gestational age in non-HIE neonates [18]. In HIE animal model studies, APT imaging was performed in a single layer at the coronal level of the basal ganglia and correlated with MRS results, which showed that APT values decreased immediately after hypoxic-ischemic injury, remaining at their lowest level for 0–2 h. Afterwards, it gradually increased and finally exceeded the control group at 48–72 h. After hypoxic-ischemic injury, lactate content increased immediately, reached the maximum level in 2–6 h, and then gradually decreased to the level of the control group.APT values were negatively correlated with lactate content. After hypoxic-ischemic injury, recovery of pH was faster than recovery of lactate homeostasis [19]; some studies have shown a transient decrease in pH after ischemic-hypoxic brain injury, followed by an increase, inducing trans-alkalosis [20]. Similarly, researchers conducted more intensive studies on the mechanisms of pH changes. Using APT imaging, brain pH level analysis, and voltage-gated proton channel (Hv1) expression analysis, they studied the regulatory mechanisms of brain pH after hypoxic-ischemic brain injury (HIBI). The research showed that Hv1 protein expression in the basal ganglia reached a peak at 0–2 h after HIBI, with significant differences from other time points. The APT values in piglets reached the lowest point at 0–2 h after HIBI, then gradually increased, and had significant differences from the control group. Brain pH decreased after HIBI, reached the lowest point at 0–2 h, and then gradually increased. Hv1 protein expression, pH, and APT values were all correlated. After hypoxic-ischemic (HI) injury, changes occurred in the brain hydrogen ions (H+) within the neural network, leading to changes in brain pH [11]. Therefore, we suggest that the increase in APTw values correlates with changes in the pH of the internal environment of the brain. In our study, the neonates underwent MRI at a time when they were no longer in the acute phase, the elevated APTw values are consistent with previous studies [9,18], and the elevated APTw values in these brain regions may be at risk of progressing to permanent damage. The brain regions with higher APTw values include the hippocampus, amygdala, caudate nucleus, and frontal lobe, all involved in cognitive and emotional processing. Changes in these areas may be closely linked to the future cognitive impairment in children with HIE.

The lower ADC values in the right anterior temporal lobe of the HIE group compared to the control group indicate restricted diffusion of water molecules in this region, suggesting microstructural changes and cellular damage. The anterior temporal lobe is involved in various cognitive functions, including memory and language processing [21–23], and its impairment can contribute to the cognitive deficits observed in children with HIE. The higher ADC values in the bilateral thalamic floor nuclei of the HIE group may reflect compensatory changes in these regions in response to the injury, as the thalamus plays a crucial role in relaying sensory and motor information to the cortex [24,25].

ROC curve analysis confirmed the diagnostic value of APTw and ADC values in identifying HIE. 20 brain regions had AUC values greater than 0.8 in the APTw analysis, and two brain regions had AUC values greater than 0.8 in the ADC analysis.The brain regions with AUCs greater than 0.8 in both the APTw and ADC analyses were right anterior temporal lobe, suggesting that the involvement of right anterior temporal lobe may be important in HIE. In furthermore, we analyzed the correlation between APTw and ADC values in each brain region. We found a significant positive correlation between APTw and ADC values in the right anterior temporal lobe. Comprehensively, the above analyses suggest that damage in right anterior temporal lobe is crucial in HIE.

The right anterior temporal lobe is involved in cognitive functions, including language processing, semantic memory, and social cognition [21,22,26–29]. Neonatal limbic system circuits are also susceptible to hypoxic-ischemic injury [30]. Our results showed an increase in APTw and a decrease in ADC values in the right anterior temporal lobe, indicating an increase in pH, the appearance of alkalosis, and cellular edema, which may be associated with metabolic disruption following hypoxia-ischemia. These changes lead to neurodegenerative damage to neurons and are tightly correlated with the neuropathophysiological mechanisms of cognitive dysfunction following HIE.

Our study also has limitations. Firstly, the sample size of our study was small, thus some confounding factors that may affect APT images were difficult to analyze statistically. There are fewer clinical studies on APT in HIE, and some studies have shown that gestational week may be related to the APT changes [18]. In our subsequent study, we will expand the sample size and include factors such as gestational week, birth weight, and mode of delivery in the analysis of the effect on APT, which will better study the changes of APT in HIE; secondly, we lacked information on follow-up. In the current prognostic assessment of APT for neurodevelopment in HIE patients, there was no significant correlation between changes in APT and neurodevelopmental assessment results [9], probably due to the short follow-up period and small sample size; whereas the prognostic assessment of ADC for neurodevelopment in HIE patients found that changes in ADC values of the basal ganglia were more sensitive to changes in ADC values than the conventional neurodevelopmental scores [6]. We need to include a long follow-up period in addition to expanding the sample size in subsequent studies to better assess neuroimaging for neurodevelopmental prognosis in HIE patients.

5. Conclusion

In conclusion, the APTw values were increased in most brain regions after hypoxia-ischemia, and more brain regions showed changes in APTw values than ADC values; hence, APT may be more sensitive to hypoxic-ischemic injury than ADC. The significant changes in the right anterior temporal lobe on APT and DWI may be closely associated with the neurological prognosis of HIE. The Results of this study show that APT and DWI play an important role in identifying and understanding the brain damage caused by HIE. Our study focused on analyzing brain changes in children with HIE with APT and ADC, and we analyzed the changes in APTw and ADC values to hypothesize the impact of factors associated with the neurodevelopmental prognosis of children with HIE. By providing meaningful insights into tissue metabolism and microstructural changes, these imaging techniques may be useful in the early diagnosis, prognosis and treatment planning of neonates with HIE.

Ethics statement

The study was ethically approved by the Ethics Committee of Wuhan Children's Hospital (2021R109-E03). Written informed consent was obtained from the parents of the participants prior to the examinations.

Data availability statement

Data will be made available on request.

Funding

This work was supported by Wuhan Municipal Health Commission under Grant WX21Z64, and Natural Science Foundation of Hubei Province under Grant 2021CFB177, Wuhan Children's Hospital under Grant 2022FEYJS002, Wuhan Clinical Research Center for Children's Medical Imaging under Grant WSTB2022-38.

CRediT authorship contribution statement

Yu Guo: Writing – original draft, Funding acquisition, Formal analysis, Data curation, Conceptualization. **Xiaohu Zhu:** Methodology, Data curation. **Jian Li:** Data curation. **Baiqi Zhu:** Data curation. **Yajing Ye:** Data curation. **Xuehua Peng:** Writing – review & editing, Supervision, Resources, Methodology, Conceptualization.

Declaration of competing interest

The authors declare that they have no known competing financial interests or personal relationships that could have appeared to influence the work reported in this paper.

References

[1] M. Douglas-Escobar, M.D. Weiss, Hypoxic-ischemic encephalopathy: a review for the clinician, JAMA Pediatr. 169 (2015) 397–403, https://doi.org/10.1001/jamapediatrics.2014.3269.
[2] J.M. Conway, B.H. Walsh, G.B. Boylan, D.M. Murray, Mild hypoxic ischaemic encephalopathy and long term neurodevelopmental outcome - a systematic review, Early Hum. Dev. 120 (2018) 80–87, https://doi.org/10.1016/j.earlhumdev.2018.02.007.
[3] A.R. Laptook, S. Shankaran, J.E. Tyson, B. Munoz, E.F. Bell, R.N. Goldberg, N.A. Parikh, N. Ambalavanan, C. Pedroza, A. Pappas, A. Das, A.S. Chaudhary, R. A. Ehrenkranz, A.M. Hensman, K.P. Van Meurs, L.F. Chalak, A.M. Khan, S.E.G. Hamrick, G.M. Sokol, M.C. Walsh, B.B. Poindexter, R.G. Faix, K.L. Watterberg, I. D. Frantz, R. Guillet, U. Devaskar, W.E. Truog, V.Y. Chock, M.H. Wyckoff, E.C. McGowan, D.P. Carlton, H.M. Harmon, J.E. Brumbaugh, C.M. Cotten, P. J. Sanchez, A.M. Hibbs, R.D. Higgins, H. Eunice Kennedy Shriver National Institute of Child, N. Human Development Neonatal Research, Effect of therapeutic hypothermia initiated after 6 hours of age on death or disability among newborns with hypoxic-ischemic encephalopathy: a randomized clinical trial, JAMA 318 (2017) 1550–1560, https://doi.org/10.1001/jama.2017.14972.
[4] Y. Dağ, A.K. Firat, H.M. Karakaş, A. Alkan, C. Yakinci, G. Erdem, Clinical outcomes of neonatal hypoxic ischemic encephalopathy evaluated with diffusion-weighted magnetic resonance imaging, Diagn Interv Radiol 12 (2006) 109–114.
[5] S. Thayyil, M. Chandrasekaran, A. Taylor, A. Bainbridge, E.B. Cady, W.K.K. Chong, S. Murad, R.Z. Omar, N.J. Robertson, Cerebral magnetic resonance biomarkers in neonatal encephalopathy: a meta-analysis, Pediatrics 125 (2010) e382–e395, https://doi.org/10.1542/peds.2009-1046.
[6] F. Cavalleri, L. Lugli, M. Pugliese, R. D'Amico, A. Todeschini, E. Della Casa, C. Gallo, R. Frassoldati, F. Ferrari, Prognostic value of diffusion-weighted imaging summation scores or apparent diffusion coefficient maps in newborns with hypoxic-ischemic encephalopathy, Pediatr. Radiol. 44 (2014) 1141–1154, https://doi.org/10.1007/s00247-014-2945-9.
[7] L. Rana, D. Sood, R. Chauhan, R. Shukla, P. Gurnal, H. Nautiyal, M. Tomar, MR Imaging of hypoxic ischemic encephalopathy - distribution Patterns and ADC value correlations, Eur J Radiol Open 5 (2018) 215–220, https://doi.org/10.1016/j.ejro.2018.08.001.
[8] K. Hayakawa, K. Tanda, S. Koshino, A. Nishimura, Z. Kizaki, K. Ohno, Pontine and cerebellar injury in neonatal hypoxic-ischemic encephalopathy: MRI features and clinical outcomes, Acta Radiol 61 (2020) 1398–1405, https://doi.org/10.1177/0284185119900442.
[9] S. Chen, X. Liu, J. Lin, Y. Mei, K. Deng, Q. Xue, X. Song, Y. Xu, Application of amide proton transfer imaging for the diagnosis of neonatal hypoxic-ischemic encephalopathy, Front Pediatr 10 (2022) 996949, https://doi.org/10.3389/fped.2022.996949.
[10] Y. Zheng, X. Wang, The applicability of amide proton transfer imaging in the nervous system: focus on hypoxic-ischemic encephalopathy in the neonate, Cell. Mol. Neurobiol. 38 (2018) 797–807, https://doi.org/10.1007/s10571-017-0552-7.
[11] Y. Zheng, X. Wang, Amide proton transfer (APT) imaging-based study on the correlation between brain pH and voltage-gated proton channels in piglets after hypoxic-ischemic brain injury, Quant. Imag. Med. Surg. 11 (2021) 4408–4417, https://doi.org/10.21037/qims-21-250.
[12] Y. Zheng, X. Wang, X. Zhao, Magnetization transfer and amide proton transfer MRI of neonatal brain development, BioMed Res. Int. 2016 (2016) 3052723, https://doi.org/10.1155/2016/3052723.
[13] J. Zhou, H.-Y. Heo, L. Knutsson, P.C.M. van Zijl, S. Jiang, APT-weighted MRI: techniques, current neuro applications, and challenging issues, J. Magn. Reson. Imag. 50 (2019) 347–364, https://doi.org/10.1002/jmri.26645.
[14] K.A. Cauley, C.G. Filippi, Apparent diffusion coefficient histogram analysis of neonatal hypoxic-ischemic encephalopathy, Pediatr. Radiol. 44 (2014) 738–746, https://doi.org/10.1007/s00247-013-2864-1.
[15] H.B. Sarnat, M.S. Sarnat, Neonatal encephalopathy following fetal distress. A clinical and electroencephalographic study, Arch. Neurol. 33 (1976) 696–705, https://doi.org/10.1001/archneur.1976.00500100030012.
[16] I.S. Gousias, A. Hammers, S.J. Counsell, L. Srinivasan, M.A. Rutherford, R.A. Heckemann, J.V. Hajnal, D. Rueckert, A.D. Edwards, Magnetic resonance imaging of the newborn brain: automatic segmentation of brain images into 50 anatomical regions, PLoS One 8 (2013) e59990, https://doi.org/10.1371/journal.pone.0059990.
[17] I.S. Gousias, A.D. Edwards, M.A. Rutherford, S.J. Counsell, J.V. Hajnal, D. Rueckert, A. Hammers, Magnetic resonance imaging of the newborn brain: manual segmentation of labelled atlases in term-born and preterm infants, Neuroimage 62 (2012) 1499–1509, https://doi.org/10.1016/j.neuroimage.2012.05.083.
[18] S. Chen, X. Liu, Y. Mei, C. Li, D. Ren, M. Zhong, Y. Xu, Early identification of neonatal mild hypoxic-ischemic encephalopathy by amide proton transfer magnetic resonance imaging: a pilot study, Eur. J. Radiol. 119 (2019) 108620, https://doi.org/10.1016/j.ejrad.2019.07.021.

[19] Y. Zheng, X.-M. Wang, Measurement of lactate content and amide proton transfer values in the basal ganglia of a neonatal piglet hypoxic-ischemic brain injury model using MRI, AJNR Am J Neuroradiol 38 (2017) 827–834, https://doi.org/10.3174/ajnr.A5066.
[20] A. Ohki, S. Saito, E. Hirayama, Y. Takahashi, Y. Ogawa, M. Tsuji, T. Higuchi, K. Fukuchi, Comparison of chemical exchange saturation transfer imaging with diffusion-weighted imaging and magnetic resonance spectroscopy in a rat model of hypoxic-ischemic encephalopathy, Magn. Reson. Med. Sci. 19 (2020) 359–365, https://doi.org/10.2463/mrms.mp.2019-0128.
[21] M.F. Bonner, A.R. Price, Where is the anterior temporal lobe and what does it do? J. Neurosci. 33 (2013) 4213–4215, https://doi.org/10.1523/JNEUROSCI.0041-13.2013.
[22] T.E. Cope, Y. Shtyrov, L.J. MacGregor, R. Holland, F. Pulvermüller, J.B. Rowe, K. Patterson, Anterior temporal lobe is necessary for efficient lateralised processing of spoken word identity, Cortex 126 (2020) 107–118, https://doi.org/10.1016/j.cortex.2019.12.025.
[23] C. Wong, J. Gallate, The function of the anterior temporal lobe: a review of the empirical evidence, Brain Res. 1449 (2012) 94–116, https://doi.org/10.1016/j.brainres.2012.02.017.
[24] M.-T. Herrero, C. Barcia, J.M. Navarro, Functional anatomy of thalamus and basal ganglia, Childs Nerv Syst 18 (2002) 386–404, https://doi.org/10.1007/s00381-002-0604-1.
[25] S.M. Sherman, Functioning of circuits connecting thalamus and cortex, Compr. Physiol. 7 (2017) 713–739, https://doi.org/10.1002/cphy.c160032.
[26] J.R. Binder, W.L. Gross, J.B. Allendorfer, L. Bonilha, J. Chapin, J.C. Edwards, T.J. Grabowski, J.T. Langfitt, D.W. Loring, M.J. Lowe, K. Koenig, P.S. Morgan, J. G. Ojemann, C. Rorden, J.P. Szaflarski, M.E. Tivarus, K.E. Weaver, Mapping anterior temporal lobe language areas with fMRI: a multicenter normative study, Neuroimage 54 (2011) 1465–1475, https://doi.org/10.1016/j.neuroimage.2010.09.048.
[27] D.F. Campos, A.R. Rocca, L.F. Caixeta, Right temporal lobe variant of frontotemporal dementia: systematic review, Alzheimer Dis. Assoc. Disord. 36 (2022) 272–279, https://doi.org/10.1097/WAD.0000000000000511.
[28] M. Irish, J.R. Hodges, O. Piguet, Right anterior temporal lobe dysfunction underlies theory of mind impairments in semantic dementia, Brain 137 (2014) 1241–1253, https://doi.org/10.1093/brain/awu003.
[29] C.C. Guo, M.L. Gorno-Tempini, B. Gesierich, M. Henry, A. Trujillo, T. Shany-Ur, J. Jovicich, S.D. Robinson, J.H. Kramer, K.P. Rankin, B.L. Miller, W.W. Seeley, Anterior temporal lobe degeneration produces widespread network-driven dysfunction, Brain 136 (2013) 2979–2991, https://doi.org/10.1093/brain/awt222.
[30] Q. Zheng, A.N. Viaene, C.W. Freeman, M. Hwang, Radiologic-pathologic evidence of brain injury: hypoperfusion in the Papez circuit results in poor neurodevelopmental outcomes in neonatal hypoxic ischemic encephalopathy, Childs Nerv Syst 37 (2021) 63–68, https://doi.org/10.1007/s00381-020-04795-0.